Title	Stability Analysis of Power Systems with Inclusion of Realistic-Modeling of WAMS Delays
Authors(s)	Liu, Muyang; Dassios, Ioannis K.; Tzounas, Georgios; Milano, Federico
Publication date	2019-01
Publication information	IEEE Transactions on Power Systems, 34 (1): 627-636
Publisher	IEEE
Item record/more information	http://hdl.handle.net/10197/9469
Publisher's statement	© 2018 IEEE. Personal use of this material is permitted. Permission from IEEE must be obtained for all other uses, in any current or future media, including reprinting/republishing this material for advertising or promotional purposes, creating new collective works, for resale or redistribution to servers or lists, or reuse of any copyrighted component of this work in other works.
Publisher's version (DOI)	10.1109/TPWRS.2018.2865559

Stability Analysis of Power Systems with Inclusion of Realistic-Modeling WAMS Delays

Muyang Liu, *Student Member, IEEE*, Ioannis Dassios, Georgios Tzounas, Federico Milano, *Fellow, IEEE*

***Abstract*— The paper studies the impact of realistic Wide-Area Measurement System (WAMS) time-varying delays on the dynamic behaviour of power systems. A detailed model of WAMS delays including pseudo-periodic, stochastic and constant components is presented. Then, the paper discusses numerical methods to evaluate the small-signal stability as well as the time-domain simulation of power systems with inclusion of such delays. The small-signal stability analysis is shown to be able to capture the dominant modes through the combination of a characteristic matrix approximation and a Newton correction technique. A case study based on the IEEE 14-bus system compares the accuracy of the small-signal stability analysis with Monte-Carlo time-domain simulations. Finally, the numerical efficiency of the proposed technique is tested through a real-world dynamic model of the all-island Irish system.**

***Index Terms*— Time-varying delay, delay differential algebraic equations (DDAEs), small-signal stability, wide-area measurement system (WAMS).**

NOTATION

a Scale factor of the Gamma distribution
$\boldsymbol{A}_0$ Conventional state matrix
$\boldsymbol{A}_i$ State matrix associated with the i-th delay
b Shape factor of the Gamma distribution
$\boldsymbol{f}$ Differential equations
$\boldsymbol{g}$ Algebraic equations
$h(\lambda)$ Comparison distributed delay term of time-varying delay
$\boldsymbol{I}$ Identity matrix
p Data packet dropout rate
T Normal delivery period for each data packet
t_k Arriving time of data packet x_k
$\boldsymbol{u}$ Discrete variables
w Weight function of time-varying delay
$\boldsymbol{x}$ State variables
x_k k-th data packet of state variable x
$\boldsymbol{y}$ Algebraic variables
α Real part of an eigenvalue
β Imaginary part of an eigenvalue
γ Adjusting coefficient of the guessed constant delay
Γ Random number following a Gamma distribution
$\Delta(\lambda)$ Characteristic equation
δt Time at which the next data packet is expected
ϵ Convergence error
$\hat{\epsilon}$ Tolerance for time domain integration algorithm
λ Eigenvalue
$\hat{\lambda}$ Corrected eigenvalue
$\boldsymbol{\nu}$ A non-trivial vector, eigenvector
$\boldsymbol{\nu}^H$ Hermitian conjugate of eigenvector $\boldsymbol{\nu}$
τ Measurement delay
$\bar{\tau}$ Mean value of τ
τ_c Initial-guess delay for the Newton correction
τ_o Constant component of the WAMS delay model
τ_p Quasi-periodic component of the WAMS delay model
τ_p' Ideal periodic component of the WAMS delay model
τ_s Stochastic component of the WAMS delay model

The authors are with the School of Electrical and Electronic Engineering, University College Dublin, Ireland. E-mails: muyang.liu@ucdconnect.ie, ioannis.dassios@ucd.ie, georgios.tzounas@ucdconnect.ie and federico.milano@ucd.ie).

This work is supported by the Science Foundation Ireland, by funding Muyang Liu, Georgios Tzounas and Federico Milano, under Investigator Programme Grant No. SFI/15/IA/3074; and Ioannis Dassios and Federico Milano, under Strategic Partnership Programme Grant No. SFI/15/SPP/E3125.

I. INTRODUCTION

A. Motivation

A Wide-Area Measurement System (WAMS) consists of a remote measurement device, e.g., a phasor measurement unit, and a communication network that transmits the measurements to a power system controller [1]. WAMSs inevitably introduce delays into the control loop and are thus potential threats to power system stability [2]. These delays are the result of a series of processes along the data communication from the measurement device to the grid, including long-distance data delivery, data packet dropout, noise, communication network congestion, etc. [3]. Due to stochastic effects and the communication mechanism, WAMS delays are necessarily time-variant. This paper proposes a detailed model of WAMS delays and numerical techniques to estimate their impact on small-signal stability and time-domain simulation of power systems.

B. Literature Review

In [2], [4]–[6], WAMS delays are regarded as constant for simplicity. A constant delay model, however, is not able to accurately define the impact of WAMS delays due to the Quenching Phenomenon (QP) [7]–[9]. QP appears for time-varying delays and consists in the change of the stability of a delay system for different delay types, even though all delays are within the same range and have the same mean value.

In [10]–[12], WAMS delays are modelled through stochastic processes. Comparing with the constant delay model, the stochastic model captures slightly better the effects of a realistic WAMS delay. Nevertheless, the stochastic model is still inaccurate as it fails to reflect the actual mechanism of WAMS delays, which include a quasi-periodic behaviour and data package dropouts. All these aspects are taken into account in this paper.

Apart from the lack of a precise WAMS delay model, a general technique to study the stability of power system with inclusion of time-varying delays is also currently missing. The most common approach is based on Lyapunov-Krasovskii Functionals (LKFs) [3], [13]–[15]. The main limit of LKFs is their numerical complexity – which prevents applications to large-size real-world power systems – and the significant conservativeness of the results [16].

Also frequency-domain approaches, including Integral Quadratic Constraintss (IQCs) [17], [18] and eigenvalue-based approach [19]–[22] have been developed. These approaches are shown to be computationally effective and accurate for large real-world power systems with inclusion of delays. Among the frequency-domain approaches, the eigenvalue-based method shows the lightest computational burden because it does not require to solve the Linear Matrix Inequalitys (LMIs) problem.

This paper further develops the eigenvalue-based techniques to solve the small-signal stability of power system by exploiting the theoretical results given in [7], [16], [23], where it is proven that time-varying delays can be approximated with summations of multiple constant delays in the linearized characteristic equation.

C. Contributions

To the best of our knowledge, this is the first attempt to propose a detailed model of realistic WAMS delays for power system applications. The specific contributions of the paper are the following:

- A realistic WAMS delay model that is able to take into account all relevant issues introduced by the WAMS communication system.
- A theorem that states the equivalence of the characteristic equations of Delay Differential Algebraic Equations (DDAEs) with fast time-varying delays and DDAEs with distributed delays.
- A discussion on how to implement the WAMS delay model in a Time Domain Integration (TDI) routine.
- A two-step numerical technique to evaluate the small-signal stability of the power system with detailed WAMS delay models. The first step utilizes the theorem above to estimate an initial guess of the eigenvalues of the DDAE; then a Newton correction method that takes into account the Probability Density Function (PDF) of the realistic WAMS delay improves the results.

D. Organization

The remainder of the paper is organized as follows. Section II briefly recalls state-of-art techniques to evaluate the small-signal stability of DDAEs and provides a general theorem to define the characteristic equation of DDAEs with time-varying delays. Section III provides a taxonomy of the components of WAMS delays and defines their numerical models. Section IV discusses the implementation of the WAMS delay model in time-domain simulation and small-signal stability analysis. Section V presents two case studies. The first one is based on IEEE 14-bus system and discusses features and limitations of the techniques described in Section IV. The second case study discusses the computational efficiency of these techniques when applied to a 1,479-bus dynamic model of the all-island Irish system. Conclusions are drawn in Section VI.

II. Small-signal Stability Analysis of DDAEs

A. DDAEs with constant delays

Power systems with inclusion of delays can be modeled as a set of DDAE in index-1 Hessenberg form [19]:

$$\begin{aligned} \dot{\boldsymbol{x}}(t) &= \boldsymbol{f}(\boldsymbol{x}(t), \boldsymbol{y}(t), \boldsymbol{x}(t-\tau), \boldsymbol{y}(t-\tau), \boldsymbol{u}(t)) \\ \boldsymbol{0} &= \boldsymbol{g}(\boldsymbol{x}(t), \boldsymbol{y}(t), \boldsymbol{x}(t-\tau), \boldsymbol{u}(t)) \ , \end{aligned} \tag{1}$$

where $\boldsymbol{u}$ models event, e.g. line outage.

To study the small-signal stability of (1), we consider its linearization at a given operating point [19]:

$$\dot{\boldsymbol{x}}(t) = \boldsymbol{A}_0 \boldsymbol{x}(t) + \sum_{i=1}^{i_{max}} \boldsymbol{A}_i (t-\tau_i) \ , \tag{2}$$

Each solution of (2) is $\boldsymbol{x}(t) = e^{-\lambda t}\boldsymbol{\nu}$. The eigenvalues are numerically equal to the roots of the characteristic equation:

$$\begin{aligned} \Delta(\lambda)\boldsymbol{\nu} &= \det \Delta(\lambda) = 0 \ , \\ \Delta(\lambda) &= \lambda \boldsymbol{I} - \boldsymbol{A}_0 - \sum_{i=1}^{v} \boldsymbol{A}_i e^{-\lambda \tau_i} \ , \end{aligned} \tag{3}$$

The solution of (3) can be approximated through an appropriate discretization [19], [24]. Reference [21] shows that the Chebyshev discretization scheme provides the best threshold between accuracy and computational burden and, hence, this is the scheme utilized in the remainder of the paper.

B. DDAEs with inclusion of time-varying delays

Reference [7] provides a theorem to transform fast time-varying periodic delays into distributed delays. By combining the mathematical proof of [7] with the definition of distributed delay given in [23], we deduce the following theorem.

Theorem 1: Consider the following linear system with time-varying delays:

$$\dot{\boldsymbol{x}}(t) = \boldsymbol{A}_0 \boldsymbol{x}(t) + \sum_{i=1}^{i_{max}} \boldsymbol{A}_i \boldsymbol{x}(t-\tau_i(t)) \ , \tag{4}$$

where $\tau_i(t) : \mathbb{R}^+ \rightarrow [\tau_{\min}, \tau_{\max}], 0 \leq \tau_{\min} < \tau_{\max}$. If the delay $\tau(t)$ changes fast enough, the small-signal stability of (4) is the same as the following *comparison system*:

$$\dot{\boldsymbol{x}}(t) = \boldsymbol{A}_0 \boldsymbol{x}(t) + \sum_{i=1}^{v} \boldsymbol{A}_i \int_{\tau_{\min}}^{\tau_{\max}} w_i(\xi) \boldsymbol{x}(t-\xi) d\xi \ , \tag{5}$$

where $w_i(\xi)$ is the PDF of the specific delay $\tau_i(t) = \xi$. The characteristic matrix of the comparison system is:

$$\Delta(\lambda) = \lambda \boldsymbol{I} - \boldsymbol{A}_0 - \sum_{i=1}^{v} \boldsymbol{A}_i h(\lambda) \ , \tag{6}$$

where

$$h(\lambda) = \int_{\tau_{\min}}^{\tau_{\max}} e^{-\lambda \xi} w(\xi) d\xi \ . \tag{7}$$

The proof of this theorem is in VI-A.

It is important to note that, for slow variations of $\tau_i(t)$, the comparison system (5) is only an approximation of (4). The stability of (4) and (5) are the same only for sufficiently high rate of change of $\tau_i(t)$. Since in physical systems the rate of change of the delays is always bounded and one cannot decide *a priori* where the threshold between *slow* and *fast* variations for a given system lays, the fidelity of the comparison system (5) can be inferred only through numerical simulations [7].

Reference [16] provides an alternative solution of (6) that consists in transforming the distributed delay into the summation of multiple constant delays and compute the eigenvalues through discretization. Although this approach can successfully solve the DDAEs with delays within specific finite range, it cannot properly handle unbounded and uncertain delays. Therefore, to develop a more general approach, we consider another eigenvalue computation technique, namely, the *Newton Correction*, which is discussed in the following subsection.

C. Newton Correction

Newton correction is a technique to refine the solution of the characteristic equation based on an appropriate initial guess, namely the eigenvalues solved through a direct approach. According to the symmetry of the eigenvalues, we only need to correct the eigenvalues $\lambda = \alpha + j\beta, \beta \geq 0$. The pseudo-code below is developed based on [20] and provides an implementation of the Newton correction specifically designed for DDAEs. *Algorithm 1:* Newton Correction for DDAEs:

1) Initialize the eigenvalue to be corrected as λ_0; the characteristic equations of targeted DDAE as $\Delta(\lambda_0)$; the maximal iteration number $k_{\max}$ and the tolerance ϵ .
2) Compute $\boldsymbol{r}_0 = \Delta(\lambda_0)$ and $\dot{\boldsymbol{r}}_0 = \frac{dr}{d\lambda}|_{\lambda=\lambda_0}$.
3) Compute an approximate eigenpair $(\lambda_0, \boldsymbol{\nu}_0)$ of the corresponding $\Delta(\lambda_0)$.
4) For $k = 1, 2, \ldots, k_{\max}$, compute:

$$\begin{bmatrix} \Delta\boldsymbol{\nu}_k \\ \Delta\lambda_k \end{bmatrix} = \begin{bmatrix} \boldsymbol{r}_k & \dot{\boldsymbol{r}}_k\boldsymbol{\nu}_k \\ \boldsymbol{\nu}_0^H & \mathbf{0} \end{bmatrix}^{-1} \begin{bmatrix} -\boldsymbol{r}_k\boldsymbol{\nu}_k \\ 1 - \boldsymbol{\nu}_0^H\boldsymbol{\nu} \end{bmatrix} ,$$

$\boldsymbol{\nu}_{k+1} = \boldsymbol{\nu}_k + \Delta\boldsymbol{\nu}_k$, and $\lambda_{k+1} = \lambda_k + \Delta\lambda_k$.

5) Compute $\boldsymbol{r}_{k+1}$ and $\dot{\boldsymbol{r}}_{k+1}$.
6) If $|\lambda_{k+1}| \leq \epsilon$ or $||\boldsymbol{r}_{k+1}||_2 \leq \epsilon$:
   stop with $\hat{\lambda} = \lambda_{k+1}$,
   otherwise: $\hat{\lambda} = \text{null}$.

Step (3) above is particularly critical for the convergence of the Newton correction algorithm. There exist a few approaches to compute an approximated the eigenvector/eigenvalue pair $(\lambda, \boldsymbol{\nu})$. These include Gaussian Elimination and Singular Value Decomposition (SVD) approach [25]. According to our tests, the SVD provides the better tradeoff between computational burden and accuracy. For this reason, all simulation results shown in the paper are based on SVD.

III. Modeling of WAMS Delays

This section describes the basic communication process of WAMSs as discussed in [26]. The WAMS delay model is deduced based on the elements that compose such a communication process. Note that, while other communication processes are possible, the elements that we consider for the WAMS delay model, namely, constant, periodic and stochastic components, are general and can be thus be utilized to define the dealys of WAMS with architectures other than the one considered in this paper.

Assume that the WAMS measures a given quantity $x(t)$ of the power system. The signal is first measured by an appropriate device and digitalized. Then the signal is processed through a data package concentrator, transmitted and finally processed through a zero-order holder (ZOH). At last, the resulting signal, say $x(t-\tau(t))$ is passed through device/controller of the power system [3]. This process is illustrated in Fig. 1.

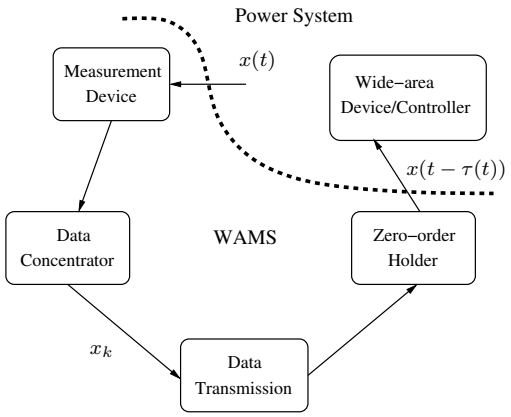

Fig. 1: WAMS elements and their interaction with the power system.

As shown in Fig. 1, the quantity collected by the measurement device $x(t)$ is concentrated and sent as digitalized data packets x_k. The data collection, concentration and processing introduce a constant delay for each packet (see Section III-B). These data packets are delivered to feed wide-area device/controller. A ZOH is implemented to avoid the potential issues resulting from the loss of data packets. The delivery of the discrete data packets leads to quasi-periodic delays, as thoroughly discussed in Subsection III-A. Apart from the two delays above, the network-induced issues, e.g., the data passing through different media, may introduce additional stochastic delays, which are also discussed in Section III-B.

A. Periodic Delay Modeling

Consider first the case of an ideal WAMS communication network. For a given medium, the delivery period of each data packet is almost the same. Then, the data packet delivery delay of such an ideal communication network can be modelled as a periodic function of time [3], as shown in Fig. 2.a. Consider a data packet arriving at $t = t_k$. The ZOH holds the data received at t_k before obtaining the next data packet; during this period, the delivery delay τ_p becomes:

$$\tau_p(t) = t - t_k \ . \tag{8}$$

Assuming that the next data packet successfully transmitted is expected to arrive at t_{k+1}, the delivery period is:

$$T = t_{k+1} - t_k \ . \tag{9}$$

In real-world WAMS communication network, the data packet can be affected by dropout and/or disorder. In this case, the ZOH holds the latest state as the feedback signal to the controllers of the power system, until the next data packet arrives successfully. Thus, a realistic data delivery delay is quasi-periodic. Figure 2.b shows the case for which one data packet x_{k+1} is lost. The probability of occurrence of a data packet dropout is called *dropout rate*, p.

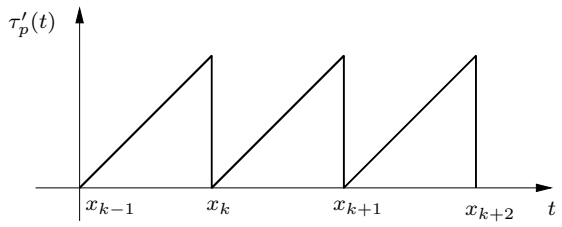

(a) Ideal delivery delay $\tau'_p(t)$

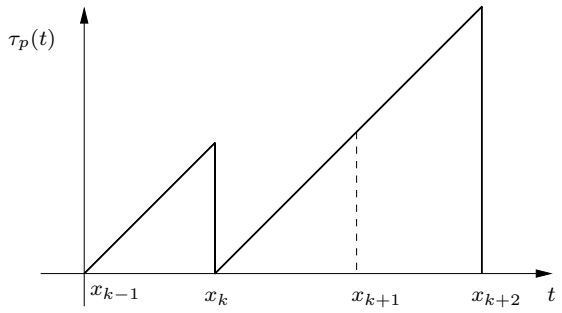

(b) Delivery delay $\tau_p(t)$ with packet dropout

Fig. 2: Time-varying delivery delay in WAMS communication network.

According to Fig. 2.b and (8), during the period that the ZOH holds in a specific status, the following condition is always satisfied:

$$\frac{d\tau_p}{dt} = 1 \ . \tag{10}$$

Then, assuming the data packet dropout rate $p \in [0, 1)$, the probability of a successful delivery is $1 - p$. A specific data packet, after a successful delivery, has the following PDF function:

$$w_p(\tau_p) = (1-p)p^n \ , \ \tau_p \in [nT, (n+1)T] \ , \ n \in \mathbb{Z} \ . \tag{11}$$

The mean value of the delivery delay according to (11) is:

$$\bar{\tau}_p = \frac{T}{2} + pT + p^2\frac{3T}{2} + \cdots + p^n\frac{(n+1)T}{2} \ . \tag{12}$$

Multiplying p on the each side of (12) leads to:

$$p\bar{\tau}_p = p\frac{T}{2} + p^2T + \cdots + p^n\frac{nT}{2} + p^{n+1}\frac{(n+1)T}{2} \ . \tag{13}$$

Then, the $\bar{\tau}_p$ can be deduced through (12)-(13):

$$\begin{aligned}(1-p)\bar{\tau}_p &= \frac{T}{2} + p\frac{T}{2} + \cdots + p^n\frac{T}{2} - p^{n+1}\frac{(n+1)T}{2} \\ &= \lim_{n\to\infty}[\frac{T(1-p^n)}{2(1-p)} - p^{n+1}\frac{(n+1)T}{2}] \\ &= \frac{T}{2(1-p)} \ .\end{aligned} \tag{14}$$

Finally, we have:

$$\bar{\tau}_p = \frac{T}{2(1-p)^2} \ . \tag{15}$$

B. Constant and Stochastic Delay Modeling

During the WAMS communication, the data collected from the measurement unit needs to be processed and exchanged through different devices [3]. In [2], it is suggested that these steps introduce a constant delay of about 75 ms for each data packet. Recent technological advances, e.g., synchronized measurement technology and real-time congestion management [27], allows reducing such a delay. Although the communication delay is fixed for each data packet, it may be slightly different for different data packets. Moreover, the network-induced issues also introduces uncertain delay during the delivery of each data packet.

Based on these considerations, apart from the quasi-periodic delay, we consider other two components in the WAMS delay model. The first is a constant delay τ_o, which is the minimal inevitable constant delay for each data packet. The second one is a stochastic delay jitter τ_s, which varies for each data packet. According to the research on the existing physical delay [28]–[30], we assume that τ_s follows a Gamma distribution. For a given packet, with the i-th dropout, one has

$$\tau_{s,i}(t) = \mathrm{Gamma}(a, b, t) \ , \tag{16}$$

Then, to account for the accumulation of the stochastic delay due to the data packet dropout, (16) is revised as:

$$\begin{aligned}\tau_s(t) = \sum_{i=0}^{\infty} p^i\tau_{s,i}(t) \ &= \frac{\mathrm{Gamma}(a, b, t)}{1-p} \\ &= \mathrm{Gamma}(\frac{a}{1-p}, b, t) \ .\end{aligned} \tag{17}$$

Then, according to Section II-B, the comparison system is:

$$\tau_s(t) = \int_0^{\infty} \frac{\xi^{b-1}e^{-\xi/\hat{a}}}{\hat{a}^b\Gamma(b)}x(t-\xi)d\xi \ , \tag{18}$$

where $\hat{a} = \frac{a}{1-p}$. Finally, the expected mean value of the Gamma distributed delay is

$$\bar{\tau}_s = \hat{a}b \ . \tag{19}$$

IV. Numerical Implementation

This section discusses the assumptions and the numerical steps required for the time domain simulation (Subsection IV-A) and small-signal stability analysis (Subsection IV-B) of power systems with WAMS delays.

A. Time-Domain Integration

A standard integration scheme, namely, the Implicit Trapezoidal Scheme (ITM), is utilized for the integration of the DDAEs modeling the power system [31]. The inclusion of constant delays in a ITM is relatively straightforward [32]. Embedding time-variant delays, however, requires special care to avoid numerical issues and guarantee accurate solutions. With this aim, we make the following assumptions:

- The occurrence of the data packet dropout is independent from the status of the last packet.
- The stochastic delay is still considered even if the data packet drops.
- The WAMS delay is represented as:

$$\tau(t) = \tau_p(t) + \tau_o + \tau_s(t) \ . \tag{20}$$

- At the initial time of the time-domain simulation, say t_0, a new data packet is delivered.

The following algorithm details the step required to generate the WAMS delay $\tau(t)$ during a time domain integration.

Algorithm 2: Time-varying WAMS delay implementation in a TDI routine:

Initialization:

Dropout rate: $p = \frac{n}{m}, n, m \in \mathbb{Z}$ and $n < m$;

Time at which the next data packet is expected to arrive: δt, note that $\delta t \in (-\infty, 0]$, where $t = 0$ is the simulation starting time;

Initial accumulated delay due to packet dropout: $\tau_{\text{drop}} := 0$;

Upper bound of stochastic delay: $\tau_s^{\max}$;

Tolerance to avoid numerical issues: $\hat{\epsilon}$;

Delay parameters: T, a, b, τ_o and initial τ_s.

For each time t_i of the time domain integration:

1) Compute $\tau_p' := \text{mod}(t_i, T)$.
2) Decide whether a data packet has arrived:
   Evaluate $\delta t > T - \hat{\epsilon}$ and $\tau_p' > T/2$.
   If *True* go to next step, else go to **Return** step.
3) Assign $\delta t := \delta t - t_i$.
4) Generate a new random value τ_s of the Gamma distribution.
5) If $\tau_s > \tau_s^{\max}$ then $\tau_s := \tau_s^{\max}$.
6) Decide whether the data packet has arrived successfully:
   Generate a random integer q, uniformely distributed in the interval $[1, m]$.
   If $q \leq n$: the data packet has arrived, then $\tau_{\text{drop}} := 0$; else: the data packet has been lost, then $\tau_{\text{drop}} := \tau_{\text{drop}} + T$ and $\tau_p := \tau_p' + \tau_{\text{drop}}$.
7) **Return**: $\tau := \tau_p + \tau_s + \tau_o$.

Each new integration time t_i is defined based on the integration time step, say Δt, as $t_i = t_{i-1} + \Delta t$. $\Delta t \ll T$ must hold. Even for small Δt, however, the calculation of τ_p' may be numerically imprecise close to zero. In step (2), therefore, we choose to capture the moment that is infinitely close to the time when $\tau_p' = \delta t = T$.

Figure 3 illustrates the time evolution of a typical WAMS delay and its components. Note that the plots in Fig. 3 are not obtained off-line but show the actual results of the time-domain simulation based on the IEEE 14-bus system that is discussed in Subsection V-A.

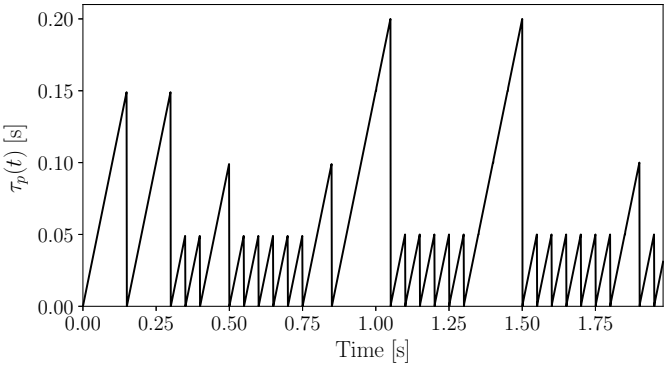

(a) Delivery delay

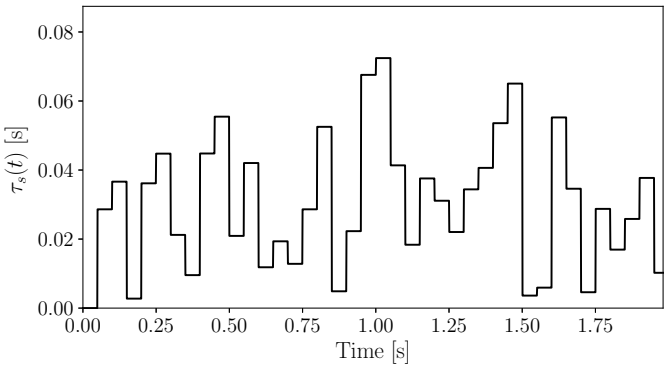

(b) Gamma distributed delay

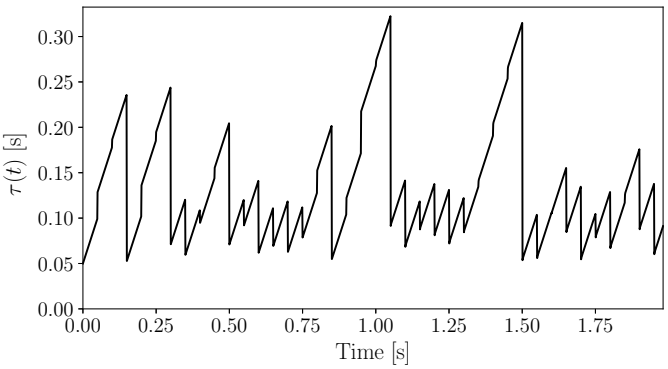

(c) WAMS delay

Fig. 3: Time evolution of a typical WAMS delay and its components. Parameters are: $\delta t = 0$ $T = 50$ ms, $\tau_o = 50$ ms, $\tau_s^{\max} = 100$ ms, $a = 0.01$, $b = 2$, $p = n/m = 3/10$, and $\hat{\epsilon} = 10^{-6}$.

B. Small-Signal Stability Analysis

The proposed small-signal stability analysis of the power system with inclusion of delay includes two major steps: (i) evaluation of an initial guess for the eigenvalues; and (ii) Newton correction based on the comparison system. For simplicity, in this section, we only discuss the implementation of the single delay case. In the case study, however, both single and multiple delay cases are considered.

First step: Choose a constant delay τ_c to replace the actual WAMS delay and solve the small-signal stability analysis through Chebyshev discretization (Section II-A). The constant delay τ_c is:

$$\tau_c = \tau_o + \gamma(\bar{\tau}_p + \bar{\tau}_s) \tag{21}$$

γ can only be found through numerical tests. Based on several simulations, we found that $\gamma \in [0.5, 2.0]$.

Second step: Set the eigenvalues obtained in the first step as the initial guesses; then solve the Newton correction (Section II-C) based on the comparison system with inclusion of the

WAMS delay. According to the previous sections, we can deduce the following characteristic equation of the system in the form of (6):

$$\det(\lambda \boldsymbol{I} - \boldsymbol{A}_0 - \boldsymbol{A}_1 h_p(\lambda) h_s(\lambda) e^{-\lambda \tau_o}) = 0 \ , \qquad (22)$$

where $h_p(\lambda)$ and $h_s(\lambda)$ are functions that adjust the characteristic equation to take into account the *distribution* of the quasi-periodic and stochastic components of the WAMS delay. For $h_p(\lambda)$, one has:

$$h_p(\lambda) = \int_0^{\infty} w_p(\xi) e^{-\lambda \xi} d\xi \ . \qquad (23)$$

Then, substituting (11) into (23):

$$\begin{aligned} h_p(\lambda) &= \int_0^T (1-p) e^{-\lambda \xi} d\xi + \int_T^{2T} (1-p) p e^{-\lambda \xi} d\xi \\ &+ \cdots + \int_{nT}^{(n+1)T} (1-p) p^n e^{-\lambda \xi} d\xi + \ldots \\ &= \frac{1-p}{\lambda} \sum_{n=0}^{\infty} p^n e^{-\lambda \xi} |_{nT}^{(n+1)T} \\ &= \frac{1-p}{\lambda} [1 + (p-1) \sum_{n=1}^{\infty} p^{n-1} e^{-n\lambda T}] \\ &= \frac{1-p}{\lambda} [1 + (p-1) \lim_{n \to \infty} \frac{e^{-\lambda T}(1 - (p e^{-\lambda T})^n)}{1 - p e^{-\lambda T}}] \\ &= \frac{1-p}{\lambda} [1 + (p-1) \frac{e^{-\lambda T}}{1 - p e^{-\lambda T}}] \ . \end{aligned} \qquad (24)$$

Similarly, according to (18), for $h_s(\lambda)$, one has:

$$\begin{aligned} h_s(\lambda) &= \int_0^{\infty} \frac{\xi^{b-1} e^{-\xi/\hat{a}}}{\hat{a}^b \Gamma(b)} e^{-\lambda \xi} d\xi \\ &= \frac{1}{\hat{a}^b \Gamma(b)} (\frac{b-1}{\xi} - \frac{1}{\hat{a}} - \lambda)^{-1} \xi^{b-1} e^{-(1/\hat{a} + \lambda)\xi} |_0^{\infty} \\ &= (1 + \hat{a}\lambda)^{-b} \ = (1 + \frac{a}{1-p} \lambda)^{-b} \ . \end{aligned} \qquad (25)$$

The deduction of (25) is given in the Appendix.

V. Case Studies

In this section, we consider two systems. The IEEE 14-bus system is utilized to discuss the accuracy and reliability of both the time-domain simulation and the small-signal stability analysis proposed in the previous sections. With this aim, we solve a sensitivity analysis for a single-delay case. The second case study is a real-world dynamic model of the Irish system, which serves to illustrate the computational burden of the proposed small-signal stability analysis.

All simulations are obtained using the Python-based software tool DOME [33]. The DOME version utilized here is based on Fedora Linux 25, Python 3.6.2, CVXOPT 1.1.9, KLU 1.3.8, and MAGMA 2.2.0. The hardware consists of two 20-core 2.2 GHz Intel Xeon CPUs, which are utilized for matrix factorization and Monte-Carlo time-domain simulations; and one NVIDIA Tesla K80 GPU, which is utilized for the small-signal stability analysis.

A. IEEE 14-bus system

This subsection investigates the feasibility and sensitivity with respect to WAMS delay parameters of the numerical approach discussed above based on IEEE 14-bus system, with a WAMS-based Power System Stabilizer (PSS) connected at generator 1 and 20% load increase. All parameters of the grid can be found in [31] and all parameters of the PSS are the same as in [16], except for the gain of the PSS that is taken as $K_w = 3.0$.

The rightmost post-contingency eigenvalues of IEEE 14-bus system following the line 2-4 outage is $-0.1366 \pm j0.0121$ if including a non-delayed PSS and $0.0352 \pm j8.8251$ without PSS. Intuitively, the system can be unstable for a delayed PSS, as the effect of the PSS is null if the delay is large enough.

Assuming that the WAMS-based PSS introduces a delay with same parameters as that of the delay $\tau(t)$ shown in Fig. 3, we investigate first the sensitivity of the system stability with respect to the data packet dropout rate p.

Four delay models with same mean value are considered:

- **M1** Realistic delay model: $\tau(t) = \tau_p(t) + \tau_o + \tau_s(t)$;
- **M2** Quasi-periodic time-varying model: $\hat{\tau}_p(t) = \tau_p(t) + \bar{\tau}_s + \tau_o$;
- **M3** Gamma distributed stochastic time-varying model: $\hat{\tau}_s(t) = \bar{\tau}_p + \tau_s(t) + \tau_o$;
- **M4** Constant delay model: $\bar{\tau} = \bar{\tau}_p + \bar{\tau}_s + \tau_o$.

The results of the small-signal stability anlaysis are shown in Table I. The eigenvalues shown in the table are the rightmost ones for the post-contingency operating point, the contingency being line 2-4 outage. The percentages shown in the rightmost column are the probability that a time-domain simulation (TDS) considering realistic delay model $\tau(t)$ (M1) is stable. 100 time-domain simulations per each value of p are solved.

According to Table I, for a fast-varying WAMS delay, the small-signal stability analysis of the comparison system indicates that the original system remains stable after the occurrence of the line outage only for small values of the dropout probability p. As p increases, the system becomes unstable. These results confirm the well-known conclusion that a fragile WAMS communication network can jeopardize the stability of the whole power system.

The different results obtained considering different delay models, namely $\tau(t)$, $\hat{\tau}_p(t)$, $\hat{\tau}_s(t)$ and $\bar{\tau}$ are typical effect of the quenching phenomenon. The WAMS delay model $\tau(t)$ and $\hat{\tau}_p(t)$ can effectively predict the small-signal stability of the system with inclusion of realistic-modeling measurement delays, while $\hat{\tau}_s(t)$ and $\bar{\tau}$ are less reliable. This indicates that the dominant effect of the delay on the system stability is caused by the quasi-periodic component. This conclusion is in accordance with the discussion in Section III.

The dropout rate sensitivity test above proves the accuracy of the small-signal stability analysis approach with a fast-varying delay. However, according to the hypothesis of comparison system (see the discussion of Theorem 1), as the data-delivery period T increases, the accuracy of the comparison system has to decrease.

Table II shows the sensitivity of the IEEE 14-bus system stability with respect to the period T, for a given dropout value,

TABLE I: Sensitivity of the data packet dropout rate p for the IEEE 14-bus system with WAMS-based PSS, $T = 50$ ms.

Parameter	Small-Signal Stability Analysis				% of stable TDI tests
p	$\tau(t)$	$\hat{\tau}_p(t)$	$\hat{\tau}_s(t)$	$\bar{\tau}$	$\tau(t)$
10%	$-0.02571 \pm j8.863470$	$-0.02630 \pm j8.863889$	$0.05227 \pm j8.818914$	$-0.13645 \pm j0.013156$	100%
20%	$-0.02100 \pm j8.867552$	$-0.02167 \pm j8.868155$	$0.05178 \pm j8.817714$	$-0.07423 \pm j10.461538$	100%
30%	$-0.01456 \pm j8.871650$	$-0.01530 \pm j8.872521$	$0.05093 \pm j8.816039$	$0.09067 \pm j10.349429$	100%
40%	$-0.00580 \pm j8.875183$	$-0.00660 \pm j8.876413$	$0.04928 \pm j8.813644$	$0.29547 \pm j10.178284$	100%
50%	$0.00583 \pm j8.876983$	$0.00513 \pm j8.878795$	$0.04576 \pm j8.810326$	$0.53497 \pm j9.908095$	95%
60%	$0.02030 \pm j8.874997$	$0.02003 \pm j8.877614$	$0.03754 \pm j8.807040$	$0.76520 \pm j9.469742$	43%
70%	$0.03590 \pm j8.866353$	$0.03684 \pm j8.869917$	$0.02030 \pm j8.814373$	$0.80451 \pm j8.762563$	5%
80%	$0.04732 \pm j8.848858$	$0.05122 \pm j8.852571$	$0.04887 \pm j8.836270$	$0.20383 \pm j10.083820$	2%
90%	$0.04409 \pm j8.827572$	$0.05144 \pm j8.824285$	$0.01770 \pm j8.827534$	$0.33595 \pm j8.469411$	1%

TABLE II: Sensitivity of the data delivery period T for the IEEE 14-bus system with WAMS-based PSS, $p = 20\%$.

Parameter	Small-Signal Stability Analysis				% of stable TDI tests
T [ms]	$\tau(t)$	$\hat{\tau}_p(t)$	$\hat{\tau}_s(t)$	$\bar{\tau}$	$\tau(t)$
10	$-0.13650 \pm j0.012863$	$-0.13655 \pm j0.012598$	$-0.13651 \pm j0.012862$	$-0.13649 \pm j0.012945$	100%
30	$-0.00732 \pm j8.850850$	$-0.00783 \pm j8.851217$	$-0.00239 \pm j9.193280$	$-0.13646 \pm j0.013108$	100%
50	$-0.02100 \pm j8.867552$	$-0.02167 \pm j8.868155$	$0.05178 \pm j8.817714$	$-0.07423 \pm j10.461538$	100%
70	$-0.03321 \pm j8.893056$	$-0.03401 \pm j8.894025$	$0.05062 \pm j8.815531$	$0.09154 \pm j10.348788$	100%
90	$-0.03799 \pm j8.919839$	$-0.03880 \pm j8.921193$	$0.04918 \pm j8.813519$	$0.23454 \pm j10.233620$	98%
110	$-0.03585 \pm j8.945412$	$-0.03658 \pm j8.947123$	$0.04747 \pm j8.811719$	$0.35650 \pm j10.118319$	19%
130	$-0.01671 \pm j8.986618$	$-0.01703 \pm j8.988843$	$0.05307 \pm j8.821853$	$0.45966 \pm j10.004321$	3%
150	$0.00442 \pm j9.006973$	$0.00447 \pm j9.009390$	$0.05300 \pm j8.821488$	$0.54616 \pm j9.892624$	0%

namely, $p = 20\%$. The results show that, for this system, the small-signal stability analysis becomes inaccurate for delays with relatively large period T, i.e., $T > 90$ ms. In this case, the time-domain simulation is thus the most reliable tool to evaluate the system stability for large values of T.

B. All-island Irish Power System with multiple delays

This subsection aims at investigating the computational burden of the numerical techniques proposed in the paper. With this aim, we consider a real-world model of the all-island Irish grid. The grid consists of 1,479 buses, 1,851 transmission lines, 245 loads, 22 conventional synchronous power plants with AVRs and turbine governors, 6 PSSs and 176 wind power plants. The topology and the steady-state operation data of the grid are provided by the Irish TSO, EirGrid. Dynamics data, however, are defined based on the technology of the generators and do not represent any actual operating condition. The topology of the Irish power system is shown in Figure 4.

We assume that the 6 PSSs are WAMS-based, each of them introduces a delay with same parameters as that shown in Fig. 3. The contingency consists in the outage of the synchronous power plant connected to bus 1378. The time step of TDI is 0.001 s. We consider two scenarios: the system with realistic low PSS gains and with high PSS gains. Both scenarios are stable if WAMS no delays are considered.

1) Scenario I: Low PSS *Gains:* In this scenario, the computational time required to calculate the initial guess of the eigenvalues is 115.8 s. Then completing the Newton correction applied to the 43 eigenvalues with $\Re(\lambda) \geq -0.3$ requires $1,309$ s.

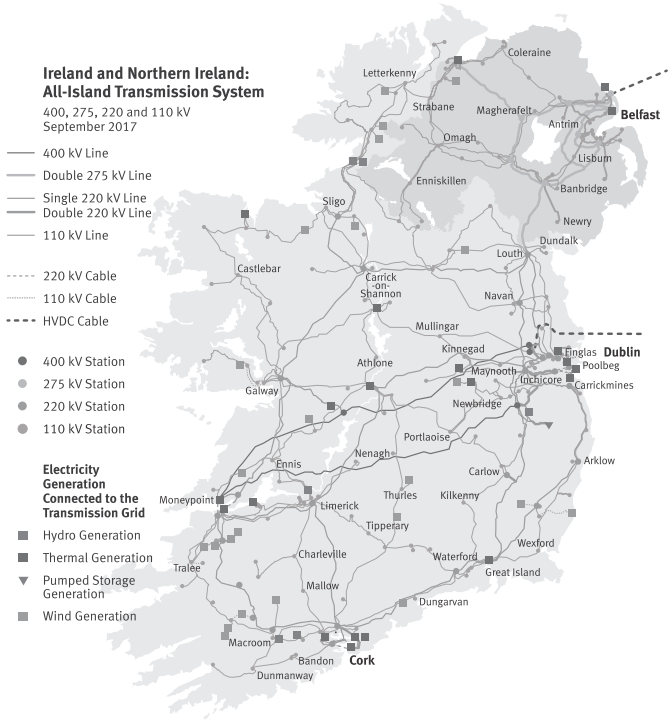

Fig. 4: All-island Irish power system map (available at: www.eirgridgroup.com).

After the completion of the Newton iteration, the 20 rightmost eigenvalues have real parts in the range $[-0.074038, -0.221988]$. As these dominant eigenvalues have negative real parts, the post-contingency grid is expected to

be stable. This conclusion is confirmed with 100 time-domain simulations, all of which are stable after the occurrence of the contingency. The computational time of each 50 s time-domain simulation ranges from 120 to 124 s. For illustration, Figure 5 shows the dynamic variation of the frequency of the Center of Inertia (COI) for one of the 100 time domain simulations.

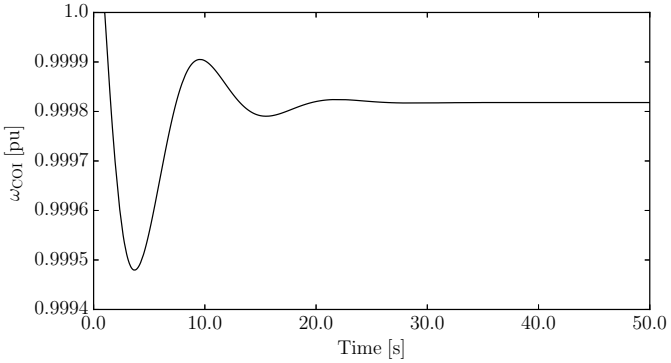

Fig. 5: Transient behaviour of the frequency of the COI for the all-island Irish grid with low PSS gains following a power plant outage.

According to simulation results, the all-island Irish system with low PSS gains is always stable and WAMS delays have no relevant impact on system stability.

2) Scenario II: High PSS *Gains:* In order to further investigate the impacts of different delay models, we increase the gains of the PSSs. This increases the damping of electromechanical oscillations but also increases the sensitivity to measurement delays. In this scenario, the computational time required to calculate the initial guess of the eigenvalues is 251.5 s. Then, completing the Newton correction applied to the 42 eigenvalues with $\Re(\lambda) \geq -0.3$ requires $1,406$ s. The 100 time domain simulations for Irish system with inclusion of WAMS delay requires about 190 s

The five rightmost eigenvalues/eigenvalue pairs of the all-island Irish system for three different case: without measurement delay, with constant delay $\bar{\tau}$ and with realistic-modelling delay $\tau(t)$ of PSS signal are shown in Table III. Figure 6 shows a typical TDI results. According to the results of the small-signal stability analysis shown in Table III, after the contingency, the system remains stable without any measurement delay, while it becomes unstable if either constant or time-varying delay is introduced. This conclusion is verified through TDI, which shows that the constant delays included in the input signals of the PSSs give birth to a small limit-cycle while the time-varying measurement delays lead to larger frequency oscillations.

VI. Conclusion

The paper proposes a detailed delay model that is able to emulate the physical behaviour of WAMS. This model allows tracking the sensitivity of the WAMS communication issues on the power system stability, e.g., the data packet dropout and data delivery period. Based on the proposed model, the paper defines both time-domain and frequency-domain techniques to evaluate the impact of WAMS delays on power system stability. These techniques are shown to be efficient and accurate for

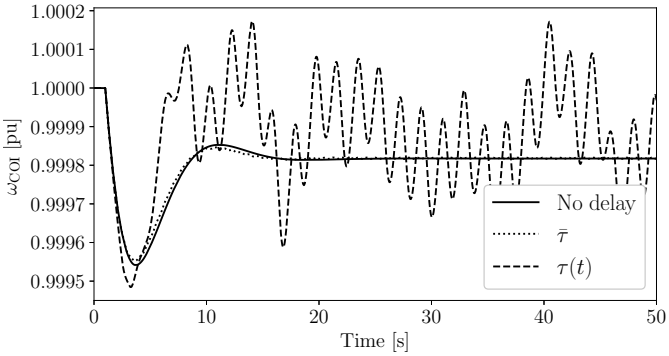

Fig. 6: Transient behavior of the frequency of the COI for the all-island Irish grid with high PSS gains following a power plant outage.

the fast-varying WAMS delays. However, both the theoretical discussion and the case study identify the limitations of the frequency-domain analysis when dealing with slow time-varying WAMS delays. The time-domain analysis is thus the only reliable tool for these cases. Future work will focus on improving the accuracy of the frequency-domain analysis for slow time-varying delays.

Appendix

A. Proof of Theorem 1

Proof: Let $\mathcal{L}\{\boldsymbol{x}(t)\} = \boldsymbol{X}(s)$ be the Laplace transform of $\boldsymbol{x}(t)$. Then, if the delays $\tau_i(t)$, $i = 1, \ldots, i_{max}$ change fast enough, s.t. we can assume a specific delay $\tau_i(t) = \xi$, by applying the Laplace transform into (2), we have

$$\mathcal{L}\{\dot{\boldsymbol{x}}(t)\} = \boldsymbol{A}_0\mathcal{L}\{\boldsymbol{x}(t)\} + \sum_{i=1}^{v} \boldsymbol{A}_i\mathcal{L}\{\boldsymbol{x}(t-\xi)\} \ .$$

By using $\mathcal{L}\{\dot{\boldsymbol{x}}(t)\} = s\boldsymbol{X}(s) - \boldsymbol{x}_0$, where $\boldsymbol{x}_0 = \boldsymbol{c}$ is the initial condition of (2) that, if not given, is equal to a constant vector $\boldsymbol{c}$; and $\mathcal{L}\{\boldsymbol{x}(t-\xi)\} = e^{-s\xi}\boldsymbol{X}(s)$ for $t \geq \xi$ and 0 for $t < \xi$; the above expression takes the form

$$s\boldsymbol{X}(s) - \boldsymbol{x}_0 = \boldsymbol{A}_0\boldsymbol{X}(s) + \sum_{i=1}^{v} \boldsymbol{A}_i e^{-s\xi}\boldsymbol{X}(s) \ ,$$

or, equivalently,

$$(s\boldsymbol{X}(s) - \boldsymbol{A}_0 - \sum_{i=1}^{v} \boldsymbol{A}_i e^{-s\xi})\boldsymbol{X}(s) = \boldsymbol{c}\boldsymbol{I} \ , \qquad (26)$$

and consequently

$$\lambda\boldsymbol{X}(s) - \boldsymbol{A}_0 - \sum_{i=1}^{v} \boldsymbol{A}_i e^{-\lambda\xi} \qquad (27)$$

is the characteristic polynomial. If we apply the Laplace transform into (5), we get

$$\mathcal{L}\{\dot{\boldsymbol{x}}(t)\} = \boldsymbol{A}_0\mathcal{L}\{\boldsymbol{x}(t)\} + \sum_{i=1}^{v} \boldsymbol{A}_i\mathcal{L}\Big\{\int_{\tau_{min}}^{\tau_{max}} w_i(\xi)\boldsymbol{x}(t-\xi)d\xi\Big\} \ ,$$

whereby using into the above expression

$$\mathcal{L}\Big\{\int_{\tau_{min}}^{\tau_{max}} w_i(\xi)\boldsymbol{x}(t-\xi)d\xi\Big\} = \mathcal{L}\{w_i(t)\}\boldsymbol{X}(s),$$

TABLE III: Rightmost eigenvalues of the all-island Irish system with high PSS gains and different delay models.

Delay model	1	2	3	4	5
No delay	-0.0958	-0.1229	$-0.1315 \pm j0.3865$	-0.1403	-0.1408
$\bar{\tau}$	$0.5403 \pm j9.3230$	-0.0958	-0.1229	$-0.1315 \pm j0.3865$	-0.1403
$\tau(t)$	$1.5949 \pm j11.1040$	-0.0958	-0.1229	-0.1408	-0.1423

and the definition of the Laplace transform of the PDF $w_i(t)$ of the specific delay ξ:

$$\mathcal{L}\{w_i(t)\} = E[e^{-s\xi}] = e^{-s\xi},$$

we obtain (26), and consequently (27). ■

B. Gamma Distributed Delay

This appendix provides the steps that lead to the deduction of (25) for the Gamma distributed delay. As a starting point, recall that well-known property that states that any PDF $f(\xi)$ must satisfy the condition [34]:

$$\int_0^\infty f(\xi)d\xi = 1 \ . \tag{28}$$

For the PDF of a Gamma distributed function $f_g(\xi)$, we have:

$$\begin{aligned}\int_0^\infty f_g(\xi,a,b)d\xi &= \int_0^\infty \frac{\xi^{b-1}e^{-\xi/\hat{a}}}{\hat{a}^b\Gamma(b)}d\xi \\ &= \frac{1}{a^b\Gamma(b)}(\frac{b-1}{\xi}-\frac{1}{a})^{-1}\xi^{b-1}e^{-\xi/a}|_0^\infty \ .\end{aligned} \tag{29}$$

Assume:

$$U(a,b) = (\frac{b-1}{\xi}-\frac{1}{a})^{-1}\xi^{b-1}e^{-\xi/a}|_0^\infty \ . \tag{30}$$

According to (28) and (29), we can expect:

$$U(a,b) = a^b\Gamma(b) \ . \tag{31}$$

Comparing (25) with (30), the $h_s(\lambda)$ can be rewritten as:

$$h_s(\lambda) = \frac{1}{\hat{a}^b\Gamma(b)}U(a_t,b) \ , \tag{32}$$

where $a_t = \frac{\hat{a}}{1+\hat{a}\lambda}$. Thus, the right-hand side of (25) is:

$$h_s(\lambda) = \frac{a_t\Gamma(b)}{\hat{a}^b\Gamma(b)} = (1+\hat{a}\lambda)^{-b} \ . \tag{33}$$

ACKNOWLEDGMENTS

The first author wishes to thank Prof. Hua Ye from Shandong University, China, for the help with the Newton correction algorithm.

REFERENCES

[1] I. Kamwa, R. Grondin, and Y. Hebert, "Wide-area measurement based stabilizing control of large power systems-a decentralized/hierarchical approach," *IEEE Trans. on Power Systems*, vol. 16, no. 1, pp. 136–153, Feb 2001.

[2] B. Naduvathuparambil, M. C. Valenti, and A. Feliachi, "Communication delays in wide area measurement systems," in *Procs of the 34th Southeastern Symposium on System Theory*, Huntsville, LA, USA, Mar. 2002.

[3] S. Wang, X. Meng, and T. Chen, "Wide-Area Control of Power Systems Through Delayed Network Communication," *IEEE Trans. on Control Systems Technology*, vol. 20, no. 2, pp. 495–503, Mar. 2012.

[4] W. Yao, L. Jiang, J. Wen, Q. H. Wu, and S. Cheng, "Wide-area damping controller of facts devices for inter-area oscillations considering communication time delays," *IEEE Trans. on Power Systems*, vol. 29, no. 1, pp. 318–329, Jan 2014.

[5] V. Bokharaie, R. Sipahi, and F. Milano, "Small-Signal Stability Analysis of Delayed Power System Stabilizers," in *Procs of the 18th Power System Computation Conference*, Wrocław, Poland, Aug. 2014.

[6] D. Dotta, A. S. e Silva, and I. C. Decker, "Wide-area measurements-based two-level control design considering signal transmission delay," *IEEE Trans. on Power Systems*, vol. 24, no. 1, pp. 208–216, Feb 2009.

[7] W. Michiels, V. V. Assche, and S. Niculescu, "Stabilization of Time-Delay Systems with a Controlled Time-Varying Delay and Application," *IEEE Trans. on Automatic Control*, vol. 50, no. 4, pp. 493–504, Apr. 2005.

[8] J. Louisell, "New examples of quenching in delay differential-delay equations having time-varying delay," in *Procs of the Fourth European Control Conference*, Karlsruhe, Germany, Sep. 1999.

[9] A. Papachristodoulou, M. M. Peet, and S. Niculescu, "Stability Analysis of Linear System with Time-Varying Delays: Delay Uncertainty and Quenching," in *Procs of the 46th IEEE Conference on Decision and Control*, New Orleans, LA. USA, Dec. 2007.

[10] J. W. Stahlhut, T. J. Browne, and G. T. Heydt, "Latency Viewed as a Stochastic Process and its Impact on Wide Area Power System Control Signals," *IEEE Trans. on Power Systems*, vol. 23, no. 1, pp. 84–91, Feb. 2008.

[11] W. Yao, L. Jiang, Q. H. Wu, J. Y. Wen, and S. J. Cheng, "Delay-Dependent Stability Analysis of the Power System With a Wide-Area Damping Controller Embedded," *IEEE Trans. on Power Systems*, vol. 26, no. 1, pp. 233–240, Feb. 2011.

[12] C. Lu, X. Zhang, X. Wang, and Y. Han, "Mathematical expectation modeling of wide-area controlled power systems with stochastic time delay," *IEEE Trans. on Smart Grid*, vol. 6, no. 3, pp. 1511–1519, May 2015.

[13] W. Yao, L. Jiang, Q. H. Wu, J. Y. Wen, and S. J. Cheng, "Delay-dependent stability analysis of the power system with a wide-area damping controller embedded," *IEEE Trans. on Power Systems*, vol. 26, no. 1, pp. 233–240, Feb 2011.

[14] W. Yao, L. Jiang, J. Wen, Q. H. Wu, and S. Cheng, "Wide-area damping controller of facts devices for inter-area oscillations considering communication time delays," *IEEE Trans. on Power Systems*, vol. 29, no. 1, pp. 318–329, Jan 2014.

[15] J. Li, Z. Chen, D. Cai, W. Zhen, and Q. Huang, "Delay-Dependent Stability Control for Power System With Multiple Time-Delays," *IEEE Trans. on Power Systems*, vol. 31, no. 3, pp. 2316–2326, May 2016.

[16] M. Liu and F. Milano, "Small-signal Stability Analysis of Power Systems with Inclusion of Periodic Time-Varying Delays," in *Procs of the 20th Power System Computation Conference*, Dublin, Ireland, June 2018.

[17] D. Cai, Q. Huang, J. Li, Z. Zhang, Y. Teng, and W. Hu, "Stabilization of time-delayed power system with combined frequency domain iqc and time domain dissipation inequality," *IEEE Trans. on Power Systems*, pre-print, 2018.

[18] P. Seiler, "Stability analysis with dissipation inequalities and integral quadratic constraints," *IEEE Trans. on Automatic Control*, vol. 60, no. 6, pp. 1704–1709, June 2015.
[19] F. Milano and M. Anghel, "Impact of Time Delays on Power System Stability," *IEEE Trans. on Circuits and Systems - I: Regular Papers*, vol. 59, no. 4, pp. 889–900, Apr. 2012.
[20] H. Ye, Y. Liu, and P. Zhang, "Efficient eigen-analysis for large delayed cyber-physical power system using explicit infinitesimal generator discretization," *IEEE Trans. on Power Systems*, vol. 31, no. 3, pp. 2361–2370, May 2016.
[21] F. Milano, "Small-Signal Stability Analysis of Large Power Systems with inclusion of Multiple Delays," *IEEE Trans. on Power Systems*, vol. 31, no. 4, pp. 3257–3266, Jul. 2016.
[22] F. Milano and I. Dassios, "Small-signal stability analysis for non-index 1 hessenberg form systems of delay differential-algebraic equations," *IEEE Trans. on Circuits and Systems - I: Regular Papers*, vol. 63, no. 9, pp. 1521–1530, Sept 2016.
[23] S. A. Campbell and R. Jessop, "Approximating the Stability Region for a Differential Equation with a Distributed Delay," *Mathematical Modelling of Natural Phenomena*, vol. 4, no. 2, pp. 1–27, 2009.
[24] D. Breda, "Solution Operator Approximations for Characteristic Roots of Delay Differential Equations," *Applied Numerical Mathematics*, vol. 56, pp. 305–317, 2006.
[25] Y. Saad, *Numerical Methods for Large Eigenvalue Problems*. Philadelphia, PA: SIAM, 2011.
[26] "Ieee standard for synchrophasor data transfer for power systems," *IEEE Std C37.118.2-2011 (Revision of IEEE Std C37.118-2005)*, pp. 1–53, Dec 2011.
[27] V. Terzija, G. Valverde, D. Cai, P. Regulski, V. Madani, J. Fitch, S. Skok, M. M. Begovic, and A. Phadke, "Wide-area monitoring, protection, and control of future electric power networks," *Procs of the IEEE*, vol. 99, no. 1, pp. 80–93, Jan 2011.
[28] L. Li, M. Fei, and X. Zhou, *Analysis on Network-Induced Delays in Networked Learning Based Control Systems*. Berlin, Heidelberg: Springer Berlin Heidelberg, 2005, pp. 310–315.
[29] C.-I. Morrescu, S.-I. Niculescu, and K. Gu, "Stability crossing curves of shifted gamma-distributed delay systems," *SIAM Journal on Applied Dynamical Systems*, vol. 6, no. 2, pp. 475–493, 2007.
[30] O. Solomon and E. Fridman, "Systems with gamma-distributed delays: A lyapunov-based analysis," in *Procs of the 52nd IEEE Conference on Decision and Control*, Dec 2013, pp. 318–323.
[31] F. Milano, *Power System Modelling and Scripting*. London: Springer, 2010.
[32] I. A. Hiskens, "Time-delay modelling for multi-layer power systems," in *Procs of ISCAS*, vol. 3, May 2003, pp. III–316–III–319 vol.3.
[33] F. Milano, "A Python-based Software Tool for Power System Analysis," in *Procs of the IEEE PES General Meeting*, Vancouver, BC, Jul. 2013.
[34] J. Chen and H. Rubin, "Bounds for the difference between median and mean of gamma and poisson distributions," *Statistics and Probability Letters*, vol. 4, no. 6, pp. 281 – 283, 1986.

Muyang Liu (S'17) received from University College Dublin, Ireland, the ME in Electrical Energy Engineering in 2016. Since September 2016, she is a Ph.D. student candidate with University College Dublin. Her scholarship is funded through the SFI Investigator Award with title "Advanced Modelling for Power System Analysis and Simulation". Her current research interests in stability analysis and robust control of power system with inclusion of measurement delays.

Ioannis Dassios received his PhD in Applied Mathematics from the Dpt of Mathematics, Univ. of Athens, Greece, in 2012. He worked as a Postdoctoral Research & Teaching Fellow in Optimization at the School of Mathematics, Univ. of Edinburgh, UK. He also worked as a Research Associate at the School of Mechanical, Aerospace and Civil Engineering, Univ. of Manchester, UK, and as a Research Fellow at MACSI, Univ. of Limerick, Ireland. He is currently a Senior Researcher at UCD Energy Institute, Univ. College Dublin, Ireland.

Georgios Tzounas (S'17) received from National Technical University of Athens, Greece, the ME in Electrical and Computer Engineering in 2017. Since September 2017, he is Ph.D. candidate with University College Dublin. His scholarship is funded through the SFI Investigator Award with title "Advanced Modelling for Power System Analysis and Simulation." His current research interests include robust control and stability analysis of time-delayed power systems.

Federico Milano (S'02, M'04, SM'09, F'16) received from the Univ. of Genoa, Italy, the ME and Ph.D. in Electrical Eng. in 1999 and 2003, respectively. From 2001 to 2002 he was with the Univ. of Waterloo, Canada, as a Visiting Scholar. From 2003 to 2013, he was with the Univ. of Castilla-La Mancha, Spain. In 2013, he joined the Univ. College Dublin, Ireland, where he is currently Professor of Power Systems Control and Protections. His research interests include power system modelling, control and stability analysis.